V European Conference on Computational Fluid Dynamics
ECCOMAS CFD 2010
J. C. F. Pereira and A. Sequeira (Eds)
Lisbon, Portugal,14-17 June 2010

NUMERICAL INVESTIGATION OF FLOW FEATURES AND ACOUSTIC RADIATION FROM ROUND CAVITIES

Olivier Marsden*, Christophe Bogey* and Christophe Bailly†

*Laboratoire de Mécanique des Fluides et d'Acoustique
UMR CNRS 5509, Ecole Centrale de Lyon, 69134 Ecully Cedex, France
e-mail: christophe.bogey@ec-lyon.fr & olivier.marsden@ec-lyon.fr
†Same address & Institut Universitaire de France
e-mail: christophe.bailly@ec-lyon.fr

Key words: Large Eddy Simulation, cavity, retroaction

Abstract. *In this paper, two Large-Eddy Simulations (LES) of cylindrical cavities of diameter 10 cm and depths 5 and 10 cm, grazed by a flow of Mach number 0.26, are reported. The incoming boundary layer is tripped, in order to reach a turbulent state upstream of the cavity. Flow and acoustic results are compared to experimental findings obtained under similar conditions, and show good similarity. The two flow velocities exhibit markedly different behaviour, the deep cavity reaching a symmetrical steady state and the shallow cavity having an asymmetrical mean flow field. The LES data are used to examine these different flow patterns.*

1 INTRODUCTION

Noise generation by flow around cylindrical cavities is currently the focus of renewed attention from a number of research teams [1, 2, 3]. In the present paper, following experimental works [2] on a cylindrical cavity grazed by a turbulent boundary layer in which both flow features and acoustic radiation were investigated for a range of Mach numbers and cavity depths, numerical studies on round cavities at full scale are reported. The cavities have a radius of $r = 5$ cm and a depth of $h = 5$ and 10 cm. The 10 cm depth configuration is considered because of the interesting far-field acoustic behaviour exhibiting two distinct peaks as shown later in the results section. The 5 cm depth cavity behaves very differently. The mean flow field observed experimentally is asymmetrical and skewed with respect to the freestream flow direction. Thus two stable antisymmetrical mean flow fields are observed. This flow behaviour is reproduced numerically, and its properties are studied.

2 PARAMETERS

The simulations are performed by solving the unsteady compressible Navier-Stokes equations using low-dispersion and low-dissipation finite-difference schemes [4]. A multi-block

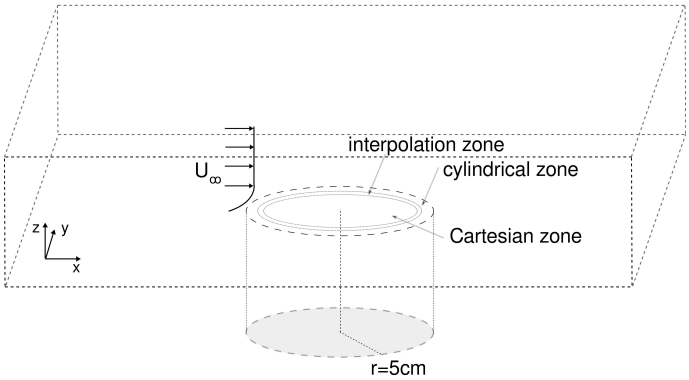

Figure 1: Sketch (not to scale) of the computational domain.

approach is followed, with cylindrical coordinates being used to represent the circular cavity wall, and Cartesian coordinates for both the centre of the cavity and the outer flow zone. Code parallelisation is based on MPI, and where necessary, inter-grid communication is carried out via optimized interpolation. The LES approach is based on the explicit application of a low-pass high-order filtering operation to the flow variables, in order to take into account the dissipative effects of the subgrid scales by relaxing turbulent energy only through the smaller scales discretized. It has been implemented with success in previous simulations of subsonic round jets [5, 6], airfoils [7] and round cavities [2]. Near boundaries, and in particular near solid walls, optimized non-centred finite-difference schemes and filters are used [8].

Figure 1 gives a sketch of the computational domain as described below. The outer computational domain covers the range $-0.36 < x < 0.52$, $-0.33 < y < 0.33$ and $0 < z < 0.48$, and is discretized by $427 \times 270 \times 102$ points in the streamwise x, cross-stream y and vertical z directions respectively. The cavity grid for the deep case contains a total of approximately 750,000 points, while the shallow cavity grid contains around 500,000 points. For both flow configurations, the upstream flow velocity is 90 m/s, and a boundary layer thickness of 17 mm is chosen, to match experimental conditions as closely as possible. A turbulent mean profile [9] is imposed at the entry, and slightly downstream of the entry plane volumetric force terms are injected in order to generate turbulent-like fluctuations in the boundary layer before it reaches the cavity. The freestream velocity and diameter-based Reynolds number for these cavity flows is $\mathrm{Re}_D = 6 \times 10^5$. For both cavity depths, the computations are run for a physical duration of 1 s, corresponding to 700,000 time steps and nine hundred convective times across the cavity opening.

For both cavity depths comparisons are made with experimental results, from Marsden *et al.* [2] for the deeper cavity, and from Hiwada *et al.* [10], Dybenko *et al.* [1] and Haigermoser *et al.* [11] for the shallower cavity.

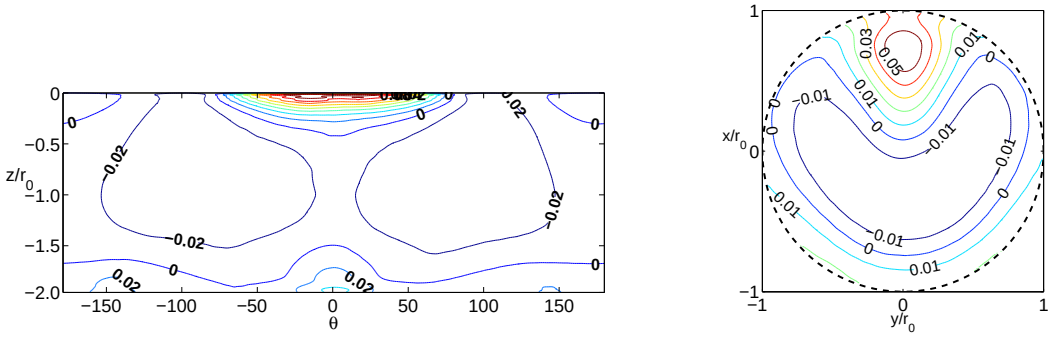

Figure 2: (left) Pressure coefficient C_p on the cylindrical cavity wall for a depth of $h = 10$ cm, as a function of polar angle θ, where $\theta = 0$ corresponds to downstream flow direction. (right) C_p on the cavity floor. Upstream flow is oriented in oriented in the x direction.

3 RESULTS

Flow and acoustic fields are described in what follows, for the deep and the shallow cavities respectively.

The flow field for the deep cavity of depth $h = 10$ cm is symmetrical, and composed mostly of a large central recirculation. The static pressure on the circular wall, represented in Figure 2 (left) as a function of vertical position z and of polar angle θ where $\theta = 0$ corresponds to the downstream flow direction, shows strong negative pockets of pressure centered around $\theta = \pm 90^o$, corresponding to the extremities of axis of rotation of the recirculating vortex that will be described below. Also visible on the static pressure plot is the intense impact zone of the shear layer on the downstream wall, around $-0.2 < z/r_0 < 0$ and $-50^o < \theta < 50^o$, where the pressure coefficient reaches a maximum value of around 0.18. Towards the bottom of the wall, three positive-pressure zones are visible, one around $\theta = 0^o$ reaching 0.04 and two around $\theta = \pm 130^o$ with a maximum of around 0.02. On the cavity floor, shown in Figure 2 (right), a characteristic horseshoe shape of negative C_p previously observed by Hiwada [10] and more recently by Marsden [2] is found. The impact of the recirculation on the floor is clearly visible with the strong positive value of $C_p = 0.06$ centred around $\theta = 0^o$ and $r/r_0 = 0.7$.

A number of streamlines associated with the mean flow field are represented in Figure 3 (left) and (right). Streamlines are coloured by the cross-stream y value of the initial seed point, from dark blue for the most negative starting y value to bright red for the most positive y value. A total of five starting points are used, all of them near the top of the cavity, spread over the range $-36^o < \theta < 36^o$. They confirm the general recirculation shape with a rotational axis parallel to y (side view), and the symmetry with respect to the $y = 0$ plane (top view). Moreover, they show a number of interesting three-dimensional features associated with the recirculating flow. The downward motion along the downstream wall is affected by the wall curvature, with streamlines first converging and then diverging as visible on the top view in Figure 3 (right). Along the bottom of the cavity the stream-

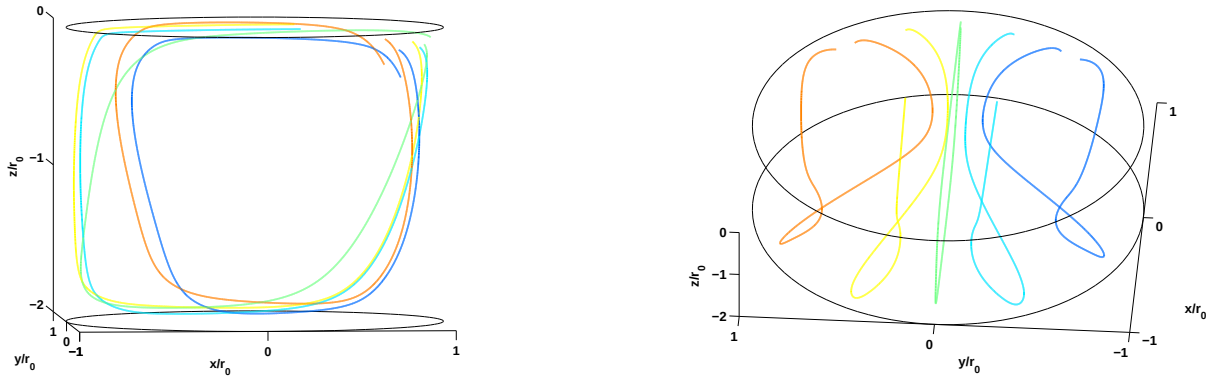

Figure 3: (left) Side view of streamlines of the mean flow field inside the cavity, coloured by initial cross-stream y coordinate. (right) Top view of streamlines of the mean flow field inside the cavity.

lines are subjected to a strong cross-stream movement, before reconverging slightly as they reascend the round wall upstream. These changes in the streamlines' directions can be qualitatively associated with the minimization of the acceleration to which the streamlines are subjected. The side view of the streamlines, represented in Figure 3 (left), shows that the recirculation shape is skewed differently in the plane of symmetry compared to away from the plane. On the $y = 0$ plane, the long axis of the ellipse-like shape (in green) is tilted forwards, while away from the plane, the long axis is tilted backwards. This suggests that the horseshoe shape observed on the static pressure in Figure 2 (right) is in fact a feature of the whole lower half, *i.e.* $z/r_0 < -1$, of the recirculation.

The acoustic radiation produced by the deep cavity with $h = 10$ cm is compared to experimental data in Figure 4. The experimental work was performed on a cavity of the same dimensions and with an incoming boundary layer of similar characteristics [2]. The plot shows the power spectral densities of the acoustic fluctuating pressure, measured for the experiment at one metre vertically above the cavity and plotted as a dashed line, and obtained from the computation 20 cm above the cavity and scaled assuming spherical wave propagation, plotted as a solid line. The two tonal peaks at frequencies of 500 and 794 Hz observed in the experiment, corresponding to diameter-based Strouhal numbers of $\mathrm{St}_D = 0.56$ and 0.88 respectively, are qualitatively reproduced. The frequency of the stronger, lower frequency peak is slightly overestimated by around 10 Hz, and its level is underestimated by approximately 8 dB. The frequency of the second peak is properly matched, while its level is underestimated by a lower margin of around 4 dB. High-frequency broadband noise is very well predicted, while lower frequency broadband noise is strongly underestimated, as can be expected for a computation with a clean incoming flow.

The shallow cavity of depth 5 cm exhibits a markedly different mean flow pattern. Indeed, despite the geometrical symmetry of the configuration, the mean flow is highly asymmetrical. This is immediately visible from the static pressure distribution on the cavity walls, presented in Figure 5 (left) and (right) for the cylindrical wall and the floor

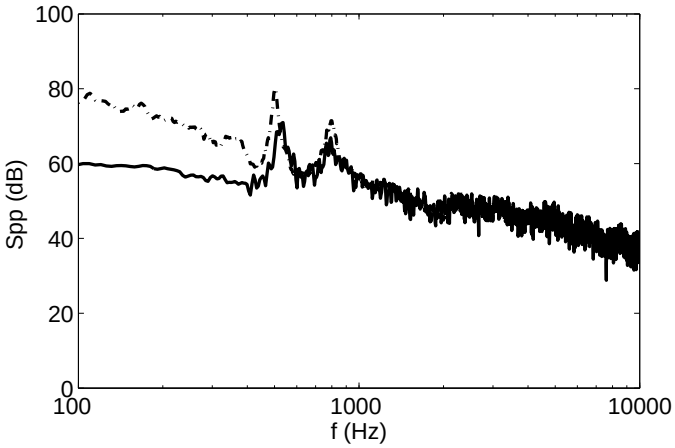

Figure 4: Sound pressure spectra ($\mathrm{Pa}^2/\mathrm{Hz}$) at 1m above the cavity for a cavity depth of $h = 10$ cm. — computed PSD, - - - measured PSD.

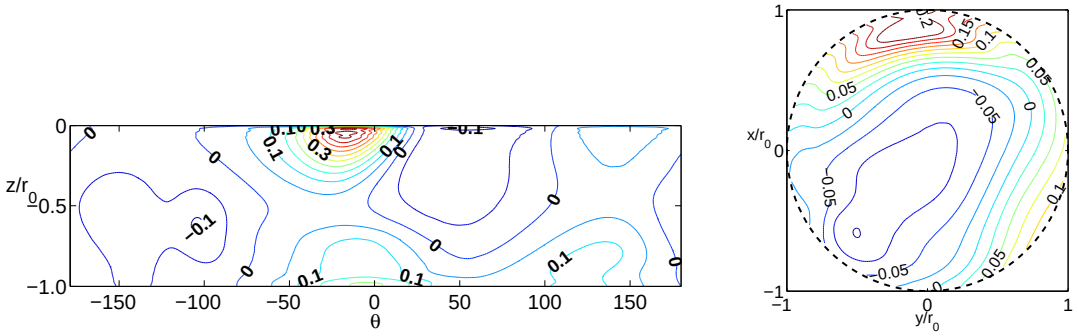

Figure 5: (left) Pressure coefficient C_p on the cylindrical cavity wall for a cavity depth of $h = 5$ cm, as a function of polar angle θ. (right) C_p on the cavity floor. Upstream flow is oriented in oriented in the x direction.

respectively. As well as being asymmetrical, static pressure levels are also much higher than for the deep cavity, reaching a maximum of 0.5, almost three times that observed previously for $h = 10$ cm, at the impact point located in this illustration around $\theta = -15^o$ and $z/r_0 = -0.06$. This translates to an unusually large drag coefficient for the shallow cavity, fact which has been known since work done on aircraft cavities in the 1970s [12]. These pressure plots are very similar to observations performed by Hiwada *et al.* [10] who measured static pressure on the walls of a cylindrical cavity with the same depth to diameter ratio, and a slightly lower Reynolds number of 1.1×10^5. The levels of C_p match well, and the general shape of the isopleths is also well recovered.

The mean flow field for this cavity depth is harder to describe than for its deeper counterpart. Mean flow components are shown in Figure 6, in the x, z and y, z planes. Of note is the very strong cross-stream $\overline{v}$ term, in both the x, z and the y, z planes. The view of the streamwize $\overline{u}$ component in the y, z plane is also interesting, as it shows a strong

deviation of the outer flow by the cavity. Over one half of the cavity, $y < 0$, the outer flow is sucked down into the cavity, which explains the very high static pressure level of $C_p = 0.5$ observed around $\theta = -15^o$ and $z/r_0 = -0.06$, and thus the abnormally high drag generated by this configuration. Over the other half of the cavity, $y > 0$, the outer mean flow is repulsed outwards, yielding a zone of low-velocity fluid above the height of the $z = 0$ wall. From these plots, it can be deduced that although a large central recirculation zone is still present, its axis of rotation is no longer aligned with the y direction but skewed strongly to one side. The streamlines represented in Figure 7 confirm this skewed nature of the recirculation, and allow the rotation to be estimated at around 35^o from the y direction. This angle can be compared that observed in the static pressure on the cavity floor, both numerically and experimentally, which is closer to 45^o. A similar trend was observed by Haigermoser *et al.* [11] who studied a cavity of comparable dimensions with tomographic and stereo PIV.

High levels of velocity fluctuations are found both in the shear layer and inside the cavity. This point is illustrated in Figure 8, which shows plots of u'_{rms}/U_∞, v'_{rms}/U_∞ and w'_{rms}/U_∞ in the x, z and y, z planes. Levels of v' and w' reach 20% of U_∞ in the shear layer, while u' attains 25%. The cross-stream views confirm the bending of the shear layer in the y direction as described for the mean streamwize flow component $\overline{u}$. Inside the cavity, background levels of fluctuations of all of the components are above 5% of the freestream velocity. A pocket of intense v' fluctuations reaching 25% of U_∞ is located around the impact zone of the shear layer, and in a small zone near the bottom of the cavity centred around $\theta = 0^o$, w' reaches 15% of U_∞.

There is no physical reason for the asymmetry to establish itself preferentially in one direction, and thus two stable mean flows, antisymmetrical with respect to the x, z plane, are anticipated. This behaviour was qualitatively reproduced by launching two independent realizations of the LES computation from an identical symmetrical flow state. The two computations yielded antisymmetrical flow fields, suggesting that numerical truncation errors are sufficient to send the computation towards one state or the other. The computational duration of one second is estimated to be substantially longer than any intrinsic time scale inherent to the configuration, thus suggesting that the computational mean flow results would not change for a longer simulation period.

The acoustic field generated by the shallow cavity is presented in Figure 9. The PSD of the computational signal recorded at 20 cm above the cavity and scaled out to 1 m (solid black line) is again compared to the corresponding experimental PSD measured at 1 m (dashed black line). Unlike the deep cavity, the shallow one does not generate strong tonal acoustic radiation, but rather a wide-band noise with a maximum around a frequency of $f = 940$ Hz. The computation captures the shape of the hump-like PSD, both in terms of frequency and of level. Frequencies above the hump are again well predicted, while lower frequencies are again underpredicted. It can be noted that neither the experimental data nor the computational wall-pressure spectra show a tonal emission around a diameter-based Strouhal number of $\mathrm{St}_D = 0.41$ such as that observed by Dybenko *et al.* [1] on a

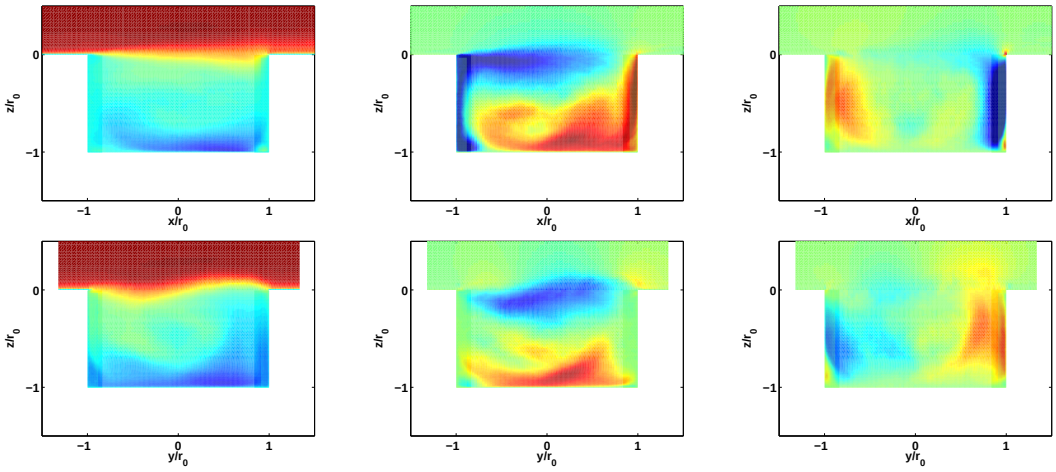

Figure 6: Mean $\overline{u}$, $\overline{v}$ and $\overline{w}$ flow components in the x, z plane, top, and the y, z plane, bottom. Colour scale between -60 and 95 m/s for $\overline{u}$, and ± 30 for $\overline{v}$ and $\overline{w}$.

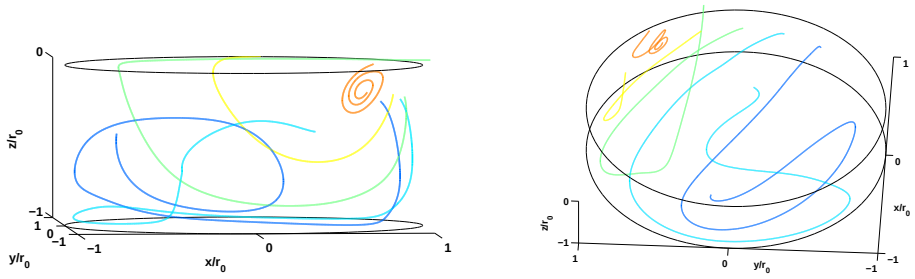

Figure 7: Side and top views of streamlines of the mean flow field inside the cavity, coloured by initial cross-stream y coordinate.

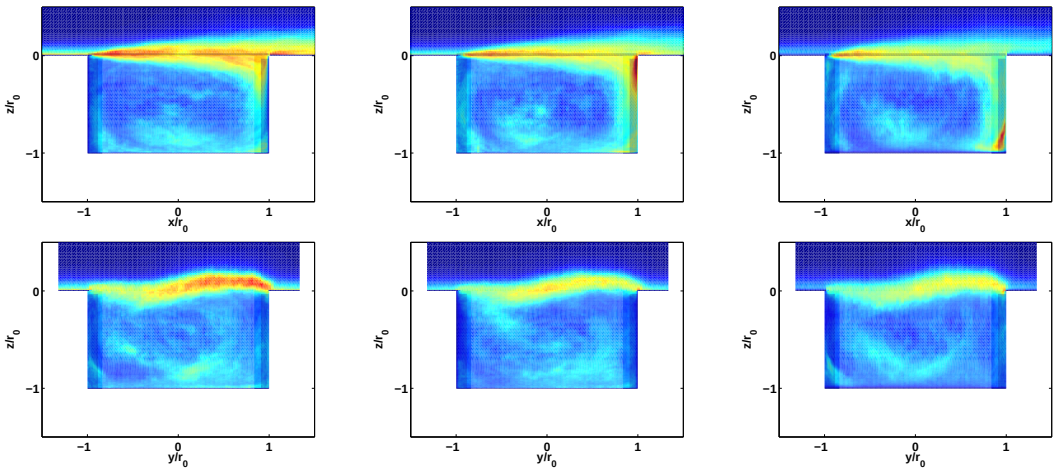

Figure 8: Fluctuation intensities u'_{rms}, v'_{rms} and w'_{rms} in the x, z plane, top, and the y, z plane, bottom, as a percentage of freestream velocity $U_\infty = 90$ m/s. Colour scale between 0 and 25%.

similar configuration. The authors of that work surmized that their observed peak was due to a fluid-dynamic Rossiter-like mechanism. They proposed that this mechanism and its associated peak might be responsible for the asymmetric mean flow. The absence of such a peak in this work, along with the high degree of observed flow asymmetry, tend to suggest that this interesting flow asymmetry has another cause.

4 CONCLUSIONS

Two cylindrical cavities of different depths grazed by a turbulent incoming boundary layer of Mach number 0.26 are studied numerically by compressible Large Eddy Simulation. For a depth to diameter ratio of 1, computational results are shown to compare well with experimental data both for the mean flow and for the radiated acoustic field. A far-field acoustic signature with two tonal peaks is quantatively reproduced. For a shallower cavity of ratio 1/2, an asymmetrical mean flow is observed. The LES computation is able to capture this interesting behaviour, and quantitative aspects of the recirculating flow are illustrated.

ACKNOWLEDGMENTS

This work was granted access to the HPC resources of the IDRIS under the allocation 2010-020204 made by GENCI (Grand Equipement National de Calcul Intensif). Some of the experimental results mentioned in this work were obtained in the context of the AERO-CAV project, financed by the french FRAE (Fondation de Recherche pour l'Aeronautique et l'Espace).

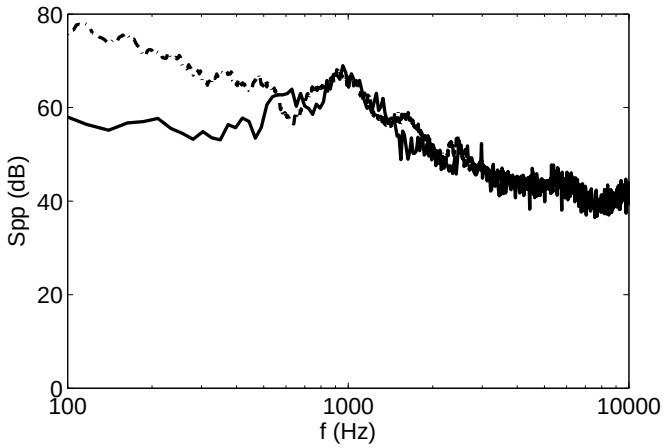

Figure 9: Sound pressure spectra (Pa^2/Hz) at 1m above the cavity for a cavity depth of $h = 5$ cm. — computed PSD, - - - measured PSD.

REFERENCES

[1] Dybenko, J. and Savory, E., "An experimental investigation of turbulent boundary layer flow over surface-mounted circular cavities," *CSME Forum*, 2006.

[2] Marsden, O., Jondeau, E., Souchotte, P., Bailly, C., Bogey, C., and Juvé, D., "Investigation of flow features and acoustic radiation of a round cavity," *AIAA Paper 2008-2851*, 2008.

[3] Mery, F., Mincu, D., and Casalis, G., "Noise Generation Analysis of a Cylindrical Cavity by LES and Global Instability," *AIAA Paper 2009-3205*, 2009.

[4] Bogey, C. and Bailly, C., "A family of low dispersive and low dissipative explicit schemes for noise computations," *Journal of Computational Physics*, Vol. 194, No. 1, 2004, pp. 194–214.

[5] Bogey, C. and Bailly, C., "Large Eddy Simulations of transitional round jets : influence of the Reynolds number on flow development and energy dissipation," *Physics of Fluids*, Vol. 18, 2006, 065101.

[6] Bogey, C. and Bailly, C., "An analysis of the correlations between the turbulent flow and the sound pressure fields of subsonic jets," *Journal of Fluid Mechanics*, Vol. 583, 2007, pp. 71–97.

[7] Marsden, O., Bogey, C., and Bailly, C., "Direct Noise Computation of the Turbulent flow around a zero-incidence airfoil," *AIAA Journal*, , No. 4, 2008, pp. 874–883.

[8] Berland, J., Bogey, C., Marsden, O., and Bailly, C., "High-order, low dispersive and low dissipative explicit schemes for multiple-scale and boundary problems," *Journal of Computational Physics*, Vol. 224, 2007, pp. 637–662.

[9] Guarini, S. E., Moser, R. D., Shariff, K., and Wray, A., "Direct numerical simulation of a supersonic turbulent boundary layer at Mach 2.5," *Journal of Fluid Mechanics*, Vol. 414, No. 1, 2000, pp. 1–33.

[10] Hiwada, M., Kawamura, T., Mabuchi, I., and Kumada, M., "Some characteristics of flow pattern and heat transfer past a circular cylindrical cavity," *Bulletin of the JSME*, Vol. 26, No. 220, October 1983.

[11] Haigermoser, C., Scarano, F., and Onorato, M., "Investigation of the flow in a circular cavity using stereo and tomographic particle image velocimetry," *Experiments in Fluids*, Vol. 46, No. 3, 2009, pp. 517–526.

[12] Gaudet, L. and Winter, K., "Measurements of the Drag of Some Characteristic Aircraft Excrescences Immersed in Turbulent Boundary Layers," Tech. Rep. TM AERO 1538, Royal Aircraft Establishment, 1973.